IEICE TRANS. COMMUN., VOL.E89–B, NO.4 APRIL 2006

PAPER

Theoretical Performance Analysis of Downlink Site Diversity in an MC-CDMA Cellular System

Arny ALI[†], *Nonmember*, **Takamichi INOUE**[†], *and* **Fumiyuki ADACHI**[†a)], *Members*

SUMMARY The downlink (base-to-mobile) bit error rate (BER) performance for a mobile user with relatively weak received signal in a multicarrier-CDMA (MC-CDMA) cellular system can be improved by utilizing the site diversity reception. With joint use of MMSE-based frequency domain equalization (FDE) and antenna diversity combining, the site diversity operation will increase the downlink capacity. In this paper, an expression for the theoretical conditional BER for the given set of channel gains is derived based on Gaussian approximation of the interference components. The local average BER is then obtained by averaging the conditional BER over the given set of channel gains using Monte-Carlo numerical method. The outage probability is measured from the numerically obtained cumulative distribution of the local average BER to determine the downlink capacity. Results from theoretical computation are compared to the results from computer simulation and discussed.

key words: *MC-CDMA, site diversity, downlink capacity, outage probability, MMSE-based FDE, antenna diversity*

1. Introduction

Due to many reflecting and refracting obstacles between a base station (BS) and a mobile user, the propagation channel suffers from a series of multipaths with different delays and amplitudes, resulting in the frequency-selective fading [1]. In addition to this, the channel is also impaired by the attenuation effect from the distance-dependent path loss and shadowing loss.

Meanwhile, multicarrier-CDMA (MC-CDMA) has been considered as a wireless access candidate for a wideband downlink transmission due to its robustness against the frequency-selectivity of the multipath channel and high frequency efficiency [2]–[8]. A basic MC-CDMA transmitter spreads the user's data symbol using an orthogonal spreading code in the frequency domain. Moreover, the use of frequency-domain equalization (FDE) based on minimum mean squared error (MMSE), referred to as MMSE-FDE in this paper, in wireless transmission has been shown to provide good bit error rate (BER) performance for an MC-CDMA system in a severe fading environment [2]–[8]. In a cellular system, MC-CDMA employs the frequency reuse feature that efficiently utilizes the limited bandwidth, similar to a direct sequence CDMA (DS-CDMA) [9]. This feature initiates the use of site diversity reception, allowing a mobile user to receive signals from multiple base stations (BS's) and thus improving the downlink transmission performance for a mobile user with relatively weak received signal power, due to the shadowing loss and distance-dependent path loss [1]. Recently, it has been shown by computer simulation in [10] that the site diversity operation can improve the downlink capacity with joint use of MMSE-FDE and receive antenna diversity. However, there has been no theoretical work to compare with the computer simulation results obtained from [10]. The objective of this paper is to build the theoretical foundation to evaluate the downlink performance with site diversity operation and compare the theoretical performance results to the computer simulation results [10].

This paper is organized as follows. Section 2 presents the downlink site diversity operation and the transmission system model for cellular MC-CDMA with MMSE-FDE and receive antenna diversity. The theoretical BER analysis is presented in Sect. 3, where the expression for conditional BER for the given set of channel gains is derived. This is followed by Sect. 4, where the local average BER is computed by averaging the conditional BER over the given set of channel gains using Monte-Carlo numerical method, and the numerically obtained cumulative distribution of the local average BER is tabulated for finding the outage probability. Theoretical computation results are then compared to computer simulation results with discussion. Section 5 gives the conclusion for this paper and some future works.

2. System Model

2.1 Site Diversity in Downlink Transmission

Assuming all BS's transmit pilot signals with equal power, a mobile user measures the local average received signal power from surrounding BS's and sorts out them out in descending order. The "local average received power" means taking the average of the instantaneous received power in order to remove the received power variations due to multipath fading and only the influence of shadowing and distance-dependent path loss remains. In site diversity operation, the selection for active BS's is performed based on a threshold P_{th}. A BS having a local average received signal power within the threshold from the maximum will be selected as an active BS for the operation. Figure 1 shows the site diversity operation model for the case of three (3) active BS's, with the radio network controller (RNC) monitoring the whole operation [10].

The threshold P_{th} can control the number of active

Manuscript received January 5, 2005.
Manuscript revised July 30, 2005.

[†]The authors are with the Department of Electrical and Communication Engineering, Graduate School of Engineering, Tohoku University, Sendai-shi, 980-8579 Japan.
a) E-mail: adachi@ecei.tohoku.ac.jp

DOI: 10.1093/ietcom/e89–b.4.1294

BS's. Therefore, it is an important design parameter in site diversity operation. When P_{th} is too small, the number of selected BS's is small and this decreases the downlink capacity. However, setting a too large P_{th} will result in selecting more BS's and increasing the interference power and for compensating this, the downlink capacity has to be reduced. Evidently, there shall be an optimum P_{th} that gives the maximum downlink capacity.

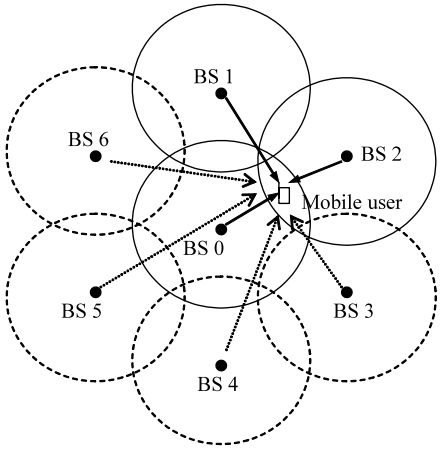

Fig. 1 Site diversity model.

2.2 Transmit/Receive Signal Representation

The downlink MC-CDMA transmitter/receiver for site diversity operation with joint use of MMSE-FDE and receive antenna diversity is illustrated in Fig. 2. An MC-CDMA system with N_c subcarriers and spreading factor SF is assumed. At BS i, the data modulated symbol sequence $\{d_{u(i)}(n);\ n = 0 \sim N_c/SF - 1\}$ for user $u(i)$ in cell of BS i is first serial-to-parallel (S/P) converted into N_c/SF parallel data sequences. Each of the S/P converter output is copied SF times and multiplied with the orthogonal spreading code $\{c_{u(i)}(k);\ k = 0 \sim SF - 1\}$. All users' spread signal components at each subcarrier are combined and multiplied with the common scrambling code $\{c_{PN(i)}(k);\ k = 0 \sim N_c - 1\}$ of BS i. Different scrambling codes are used in different cell sites for separating the cell sites as in DS-CDMA cel-

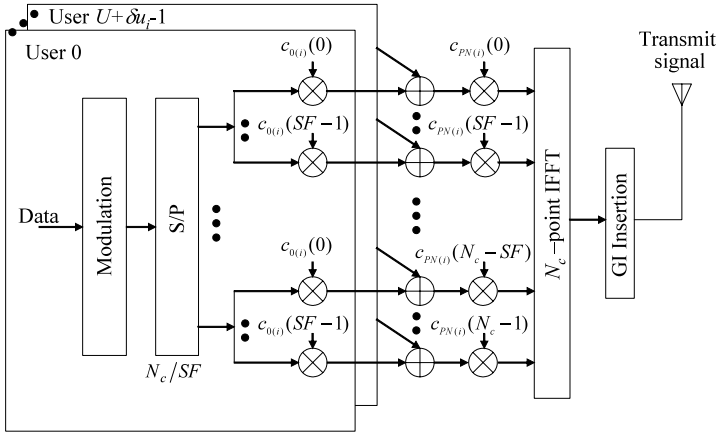

(a) Base station transmitter.

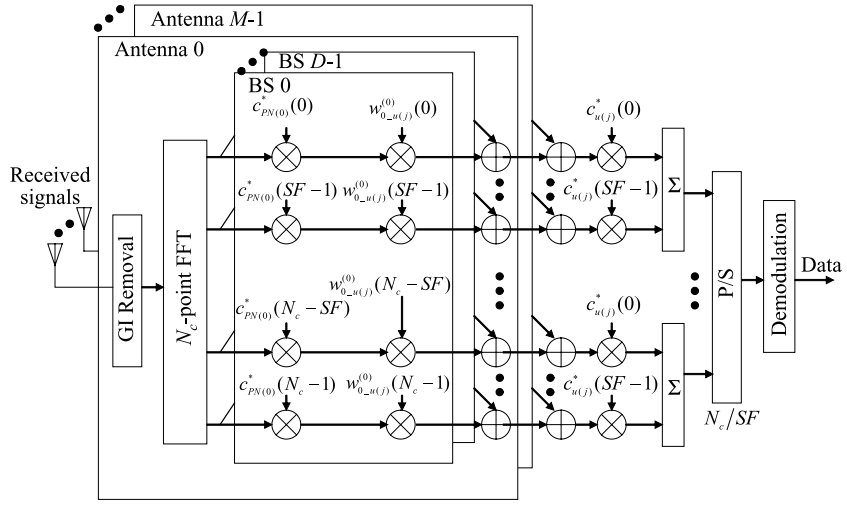

(b) Mobile station receiver.

Fig. 2 Downlink MC-CDMA transmitter/receiver with site diversity operation.

lular systems [11], besides making the resultant signal to be white-noise like.

In this paper, we use discrete-time representation of the transmit signal. The composite transmit signal of BS i at subcarrier k is given as

$$\tilde{s}_i(k) = \sqrt{\frac{2P_i}{SF}} \sum_{u(i)=0}^{U+\delta u_i-1} d_{u(i)} \left(\left\lfloor \frac{k}{SF} \right\rfloor \right) \times c_{u(i)}(k \bmod SF) c_{PN(i)}(k) \quad (1)$$

with P_i and $U + \delta u_i$ defined as the transmit power per channel and the total number of active channels (users) of BS i, respectively, where U denotes the number of users per cell and δu_i denotes the number of additional channels of BS i for site diversity (for users, in surrounding cells, receiving signals from BS i during site diversity operation) and $\left|d_{u(i)}(n)\right| = \left|c_{u(i)}(k)\right| = \left|c_{PN(i)}(k)\right|$=1. The orthogonal spreading and the scrambling codes have the following characteristics

$$\begin{cases} \dfrac{1}{SF} \displaystyle\sum_{k=0}^{SF-1} c_{u(i)}(k) c^*_{u'(i)}(k) = \delta(u - u') \\ E\left[c_{PN(i)}(k) c^*_{PN(i)}(k') \right] = \delta(k - k') \end{cases}, \quad (2)$$

where $\delta(.)$ denotes the delta function.

Perfect orthogonality between users cannot be achieved in a multipath fading channel, and this produces the multiple access interference (MAI). Furthermore, the inter-cellular interference (ICI) from other neighboring cells has to be considered since the scrambling codes between cells are not orthogonal. After N_c-point IFFT, an N_g-sample cyclic prefix is inserted into the guard interval (GI) placed at the beginning of each symbol frame to mitigate the inter-symbol interference (ISI). The MC-CDMA transmit signal is then expressed as

$$s_i(t) = \sum_{k=0}^{N_c-1} \tilde{s}_i(k) \exp\left(j2\pi k \frac{t}{N_c} \right) \quad (3)$$

for $t = -N_g \sim N_c - 1$.

We consider user $u(j)$ in cell of BS j as a user of interest. The signal $s_i(t)$ transmitted from BS i is assumed to go through a frequency-selective block Rayleigh fading channel with L independent propagation paths. The channel impulse response observed by antenna m can be written as [12]

$$h^{(m)}_{i\_u(j)}(\tau) = \sum_{l=0}^{L-1} \xi^{(m)}_{i\_u(j),l} \delta(\tau - \tau_l), \quad (4)$$

where $\xi^{(m)}_{i\_u(j),l}$ and τ_l denotes the complex path gain and time delay of the path l between BS i and antenna m of user $u(j)$ in cell of BS j respectively, with $E\left[\sum_{l=0}^{L-1} \left| \xi^{(m)}_{i\_u(j),l} \right|^2 \right] = 1$ for all m, with E[.] representing the ensemble average operation. It is assumed that the time delay of each path is an integer multiple of the N_c-point IFFT sampling period T_c. For M-branch antenna diversity reception, the antenna separation is assumed to be sufficiently large for all the receiving antennas to obtain independent fading and the path gains $\{\xi^{(m)}_{i\_u(j),l}; m = 0, \ldots, M-1, l = 0, \ldots, L-1\}$ are then characterized to be independent zero-mean complex random processes.

The MC-CDMA signal transmitted from a base station goes through a frequency-selective fading channel. The received MC-CDMA signal at antenna m of user $u(j)$ in cell of BS j is sampled at a rate of $1/T_c$. Its equivalent baseband representation, $r^{(m)}_{u(j)}(t)$, $t = -N_g \sim N_c - 1$, is given by

$$r^{(m)}_{u(j)}(t) = \sum_{i=0}^{\infty} \sum_{l=0}^{L-1} \xi^{(m)}_{i\_u(j),l} s_{i\_u(j)}(t - \tau_l) + n^{(m)}(t), \quad (5)$$

where $s_{i\_u(j)}(t)$ denotes the MC-CDMA signal transmitted from BS i (i.e., $s_i(t)$ in (3)) and received by user $u(j)$ in cell of BS j and $n^{(m)}(t)$ is the zero-mean complex additive white Gaussian noise (AWGN) having a variance of $2N_0/T_c$ with N_0 being the single-sided power spectrum density. $s_{i\_u(j)}(t)$ is given as

$$\begin{cases} s_{i\_u(j)}(t) = \sqrt{\dfrac{S_{i\_u(j)}}{P_i}} s_i(t) \\ S_{i\_u(j)} = P_i \times r^{-\alpha}_{i\_u(j)} \times 10^{-\eta_{i\_u(j)}/10} \end{cases}, \quad (6)$$

where $S_{i\_u(j)}$ represents the local average signal power received by user $u(j)$ from BS i, $r_{i\_u(j)}$ and $\eta_{i\_u(j)}$ respectively the distance and the shadowing loss in dB between the BS i and user $u(j)$, and α the path loss exponent. Since the shadowing loss varies following to approximately the lognormal distribution [1], $\eta_{i\_u(j)}$ is characterized as a zero-mean Gaussian variable with the standard deviation β.

After the GI is removed with the assumption that there is no exceeding time delay, the received signal at each antenna is decomposed into N_c-subcarrier components by the FFT processing. The kth subcarrier component is given as

$$\begin{aligned} R^{(m)}_{u(j)}(k) &= \frac{1}{N_c} \sum_{t=0}^{N_c-1} r^{(m)}_{u(j)}(t) \exp\left(-j2\pi k \frac{t}{N_c} \right) \\ &= \left[\sum_{i=0}^{\infty} H^{(m)}_{i\_u(j)}(k) \sqrt{\frac{2S_{i\_u(j)}}{SF}} \times \left(\sum_{u(i)=0}^{U+\delta u_i-1} d_{u(i)} \left(\left\lfloor \frac{k}{SF} \right\rfloor \right) c_{u(i)}(k \bmod SF) c_{PN(i)}(k) \right) \right] + \prod^{(m)}(k), \end{aligned} \quad (7)$$

where $H^{(m)}_{i\_u(j)}(k)$ and $\Pi^{(m)}(k)$ are respectively the channel gain and the noise component due to AGWN received on antenna m and they are given as

$$\begin{cases} H^{(m)}_{i\_u(j)}(k) = \displaystyle\sum_{l=0}^{L-1} \xi^{(m)}_{i\_u(j),l} \exp\left(-j2\pi k \frac{\tau_l}{N_c} \right) \\ \Pi^{(m)}(k) = \dfrac{1}{N_c} \displaystyle\sum_{t=0}^{N_c-1} n^{(m)}(t) \exp\left(-j2\pi k \frac{t}{N_c} \right) \end{cases}. \quad (8)$$

2.3 Joint MMSE-FDE and Receive Antenna Diversity

The N_c-subcarrier components are multiplied by the complex conjugate of the scrambling code to extract the desired signal component from the selected active BS in the site diversity operation. To reduce the distortion among subcarrier components arising from frequency-selective fading, the frequency domain equalization is necessary [2], [3]. The MMSE weight for the joint FDE and receive antenna diversity derived in site diversity operation is given as [10]

$$w_{i\_u(j)}^{(m)}(k) = \frac{\Gamma_{i\_u(j)}^{eff} H_{i\_u(j)}^{(m)*}(k)}{\sum_{i=0}^{\infty}(U+\delta u_i)\Gamma_{i\_u(j)}^{eff}\sum_{m=0}^{M-1}\left|H_{i\_u(j)}^{(m)}(k)\right|^2 + SF} \tag{9}$$

with

$$\begin{aligned}\Gamma_{i\_u(j)}^{eff} &= \frac{S_{i\_u(j)}N_cT_c}{N_0} \\ &= \frac{E_s}{N_0}\times r_{i\_u(j)}^{-\alpha}\times 10^{-\eta_{i\_u(j)}/10},\end{aligned} \tag{10}$$

where $E_s/N_0 = P_iN_cT_c/N_0$ represents the transmitted effective symbol energy-to-AWGN power spectrum density ratio. Then, the signal components of each subcarrier k received by M antennas are all combined.

2.4 Decision Variable

To obtain the decision variable $y_{u(j)}(n)$ for the nth data modulated symbol of user $u(j)$, site diversity combining (i.e., combining the desired signal kth subcarrier components received from D selected BS's) is performed first after joint FDE and receive diversity [10] and then, despreading (i.e., summing up the site diversity-combined kth subcarrier component from $k{=}nSF$ to $(n{+}1)SF{-}1$ after multiplying with the complex conjugate of the spreading code $c_{u(j)}(k \bmod SF)$). The decision variable is expressed as

$$\begin{aligned}&y_{u(j)}(n) \\ &= \frac{1}{SF}\sum_{k=nSF}^{(n+1)SF-1}\left(\sum_{m=0}^{M-1}\sum_{b=0}^{D-1}\varepsilon_b w_{b\_u(j)}^{(m)}(k)R_{u(j)}^{(m)}(k)c_{PN(b)}^*(k)\right) \\ &\quad\times c_{u(j)}^*(k \bmod SF)\end{aligned} \tag{11}$$

where D is the allowable maximum number of active BS's and $\varepsilon_b{=}1$ (0) for the BS with $\Delta_b < P_{\text{th}}$ (otherwise) with Δ_b representing the difference of the local average received signal power associated with BS_b from the maximum value. The active BS index is given in descending order and only D strongest BS's that satisfy $\Delta_b < P_{\text{th}}$ are selected for site diversity operation [10].

After the parallel-to-serial (P/S) conversion, the set of N_c/SF decision variables is demodulated to recover the transmitted data symbol sequence. Substituting (6) into (11) gives

$$y_{u(j)}(n) = x_{u(j)}(n) + \mu_{noise}(n) + \mu_{MAI}(n) + \mu_{ICI}(n), \tag{12}$$

where the first term represents the desired signal component, the second term the noise component due to AWGN, the third term the MAI and the fourth term the ICI. The desired signal component is given by

$$\begin{aligned}&x_{u(j)}(n) \\ &= \left(\frac{1}{SF}\sum_{k=nSF}^{(n+1)SF-1}\sum_{m=0}^{M-1}\sum_{b=0}^{D-1}\varepsilon_b w_{b\_u(j)}^{(m)}(k)\sqrt{\frac{2S_{b\_u(j)}}{SF}}H_{b\_u(j)}^{(m)}(k)\right) \\ &\quad\times d_{u(j)}(n)\end{aligned} \tag{13}$$

whereas the noise component is given as

$$\begin{aligned}\mu_{noise}(n) &= \frac{1}{SF}\sum_{k=nSF}^{(n+1)SF-1}\sum_{m=0}^{M-1}\sum_{b=0}^{D-1}\varepsilon_b w_{b\_u(j)}^{(m)}(k) \\ &\quad\times c_{PN(b)}^*(k)c_{u(j)}^*(k \bmod SF)\prod^{(m)}(k)\end{aligned} \tag{14}$$

the MAI as

$$\begin{aligned}&\mu_{MAI}(n) \\ &= \frac{1}{SF}\sum_{k=nSF}^{(n+1)SF-1}\sum_{m=0}^{M-1}\sum_{b=0}^{D-1}\sum_{\substack{u(b)=0\\ \neq u(j)}}^{U+\delta u_b-1}\varepsilon_b\sqrt{\frac{2S_{b\_u(j)}}{SF}}\tilde{H}_{b\_u(j)}^{(m)}(k) \\ &\quad\times c_{u(b)}(k \bmod SF)c_{u(j)}^*(k \bmod SF)d_{u(b)}(n)\end{aligned} \tag{15}$$

with $\tilde{H}_{b\_u(j)}^{(m)}(k) = w_{b\_u(j)}^{(m)}(k)H_{b\_u(j)}^{(m)}(k)$, and the ICI as

$$\begin{aligned}&\mu_{ICI}(n) \\ &= \frac{1}{SF}\sum_{k=nSF}^{(n+1)SF-1}\sum_{m=0}^{M-1}\sum_{b=0}^{D-1}\sum_{\substack{i=0\\ \neq b}}^{\infty}\sum_{u(i)=0}^{U+\delta u_i-1}\varepsilon_b\sqrt{\frac{2S_{i\_u(j)}}{SF}}H_{i\_u(j)}^{(m)}(k) \\ &\quad\times w_{b\_u(j)}^{(m)}(k)c_{PN(i)}(k)c_{PN(b)}^*(k) \\ &\quad\times c_{u(i)}(k \bmod SF)c_{u(j)}^*(k \bmod SF)d_{u(i)}(n)\end{aligned} \tag{16}$$

3. BER Analysis

This section consists of the derivation of the theoretical conditional SINR and the conditional BER for the MC-CDMA downlink, which are based on Gaussian approximation of the interference components, MAI and ICI. The Gaussian approximation is established based on the central limit theorem [13].

3.1 Derivation of SINR

It is understood from (12) that the output of the despreader, $y_{u(j)}(n)$ is a random variable with mean $x_{u(j)}(n)$ conditioned on $\{H_{i\_u(j)}^{(m)}(k)\}$. The users' binary data and the scrambling code are assumed to be independently and identically distributed (i.i.d.) random variables taking values $\{+1, -1\}$ with equal probability. The orthogonal spreading code also takes the values $\{+1, -1\}$ with equal probability. Using the central

limit theorem, the MAI and ICI components can be approximated to be zero-mean complex-valued Gaussian noise for a large number of users. Consequently, the sum of μ_{noise}, μ_{MAI} and μ_{ICI} can be treated as a new zero-mean complex-valued Gaussian noise μ. The sum of the variances from the AWGN noise, MAI and ICI gives the variance for μ, which is given by

$$2\sigma_{\mu}^2 = E[|\mu|^2] = 2\sigma_{noise}^2(n) + 2\sigma_{MAI}^2(n) + 2\sigma_{ICI}^2(n). \quad (17)$$

The variances of the noise, MAI and ICI components in (17) can be separately derived. From (15), the term μ_{MAI} can be rewritten as

$$\begin{aligned}&\mu_{MAI}(n)\\ &= \frac{1}{SF}\sum_{k=nSF}^{(n+1)SF-1}\sum_{b=0}^{D-1}\varepsilon_b\left\{\hat{H}_{b\_u(j)}(k) - \bar{H}_{b\_u(j)}(n) + \bar{H}_{b\_u(j)}(n)\right\}\\ &\times\sqrt{\frac{2S_{b\_u(j)}}{SF}}\sum_{\substack{u(b)=0\\ \neq u(j)}}^{U+\delta u_b-1} d_{u(b)}(n)\, c_{u(b)}(k \bmod SF)c_{u(j)}^*(k \bmod SF)\end{aligned} \quad (18)$$

with

$$\begin{cases}\hat{H}_{b\_u(j)}(k) = \sum_{m=0}^{M-1} w_{b\_u(j)}^{(m)}(k)H_{b\_u(j)}^{(m)}(k)\\ \bar{H}_{b\_u(j)}(n) = \frac{1}{SF}\sum_{k=nSF}^{(n+1)SF-1}\hat{H}_{b\_u(j)}(k)\end{cases}, \quad (19)$$

Since the orthogonal spreading codes are used, then

$$\sum_{k=nSF}^{(n+1)SF-1} c_{u(b)}(k \bmod SF)c_{u(j)}^*(k \bmod SF) = 0 \quad (20)$$

for $u(b) \neq u(j)$. Using (20), we have

$$\begin{aligned}&\frac{1}{SF}\sum_{k=nSF}^{(n+1)SF-1}\sum_{b=0}^{D-1}\varepsilon_b\bar{H}_{b\_u(j)}(n)\sqrt{\frac{2S_{b\_u(j)}}{SF}}\\ &\times\sum_{\substack{u(b)=0\\ \neq u(j)}}^{U+\delta u_b-1} d_{u(b)}(n)c_{u(b)}(k \bmod SF)c_{u(j)}^*(k \bmod SF) = 0\end{aligned} \quad (21)$$

in (18). Therefore, (18) reduces to

$$\begin{aligned}&\mu_{MAI}(n)\\ &= \frac{1}{SF}\sum_{k=nSF}^{(n+1)SF-1}\sum_{b=0}^{D-1}\varepsilon_b\left\{\hat{H}_{b\_u(j)}(k) - \bar{H}_{b\_u(j)}(n)\right\}\\ &\times\sqrt{\frac{2S_{b\_u(j)}}{SF}}\sum_{\substack{u(b)=0\\ \neq u(j)}}^{U+\delta u_b-1} d_{u(b)}(n)\\ &c_{u(b)}(k \bmod SF)c_{u(j)}^*(k \bmod SF).\end{aligned} \quad (22)$$

Since different users' transmitting data symbols are independent, i.e., $E[d_{u(b)}(n)d_{u'(b')}^*(n)] = 1(0)$ if $u(b) = u'(b')$ (otherwise), the variance of the MAI component can be given as

$$\begin{aligned}&2\sigma_{MAI}^2(n)\\ &= E[|\mu_{MAI}(n)|^2]\\ &= \frac{2}{SF^2}\sum_{b=0}^{D-1}\varepsilon_b S_{b\_u(j)}(U + \delta u_b - 1)\\ &\times\frac{1}{SF}\sum_{k=nSF}^{(n+1)SF-1}\left|\hat{H}_{b\_u(j)}(k) - \bar{H}_{b\_u(j)}(n)\right|^2.\end{aligned} \quad (23)$$

Further simplification can be made using (19) as

$$\begin{aligned}&2\sigma_{MAI}^2(n) = \frac{2}{SF^2}\sum_{b=0}^{D-1}\varepsilon_b S_{b\_u(j)}(U + \delta u_b - 1)\\ &\times\left\{\frac{1}{SF}\sum_{k=nSF}^{(n+1)SF-1}\left|\hat{H}_{b\_u(j)}(k)\right|^2 - \left|\frac{1}{SF}\sum_{k=nSF}^{(n+1)SF-1}\hat{H}_{b\_u(j)}(k)\right|^2\right\}.\end{aligned} \quad (24)$$

Next, the variance of the ICI component is obtained from (16). Since random scrambling codes is assumed (i.e., $E[c_{PN(b)}^*(k)c_{PN(b')}(k)] = 1(0)$ if $b = b'$ and $k = k'$ (otherwise)), the variance of the ICI component can be approximated as

$$\begin{aligned}&2\sigma_{ICI}^2(n) = E[|\mu_{ICI}(n)|^2]\\ &= \frac{2}{SF^2}\sum_{b=0}^{D-1}\varepsilon_b\sum_{\substack{i=0\\ \neq b}}^{\infty} S_{i\_u(j)}(U + \delta u_i)\\ &\times\frac{1}{SF}\sum_{k=nSF}^{(n+1)SF-1}\sum_{m=0}^{M-1}\sum_{m'=0}^{M-1}\left\{w_{b\_u(j)}^{(m)}(k)w_{b\_u(j)}^{(m')*}(k)\right\}\\ &\times\left\{H_{i\_u(j)}^{(m)}(k)H_{i\_u(j)}^{(m')*}(k)\right\}.\end{aligned} \quad (25)$$

Since $\{H_{i\_u(j)}^{(m)}(k);\ m = 0 \sim M-1\}$ are independent zero-mean variables, the sum of ICI components from different interfering cells, except for the case of $m = m'$, can be approximated to be zero from the law of large numbers [13] for a large number of interfering cells. Therefore, we have

$$\begin{aligned}&2\sigma_{ICI}^2(n) = \frac{2}{SF^2}\sum_{b=0}^{D-1}\sum_{\substack{i=0\\ \neq b}}^{\infty}\varepsilon_b S_{i\_u(j)}(U + \delta u_i)\\ &\times\frac{1}{SF}\sum_{k=nSF}^{(n+1)SF-1}\sum_{m=0}^{M-1}\left|w_{b\_u(j)}^{(m)}(k)H_{i\_u(j)}^{(m)}(k)\right|^2.\end{aligned} \quad (26)$$

Finally, the variance of the noise term is obtained from (14). For the random scrambling codes, the variance of the noise component is given as

$$\begin{aligned}&2\sigma_{noise}^2(n) = \frac{1}{SF^2}\sum_{b=0}^{D-1}\varepsilon_b\sum_{k=nSF}^{(n+1)SF-1}\sum_{m=0}^{M-1}\sum_{m'=0}^{M-1}\left\{w_{b\_u(j)}^{(m)}(k)w_{b\_u(j)}^{(m')*}(k)\right\}\\ &\times E\left[\prod^{(m)}(k)\prod^{(m')*}(k)\right].\end{aligned} \quad (27)$$

Since noise components on the different antennas are independent (i.e., $E[\prod^{(m)}(k)\prod^{(m')}(m)] = 2N_0/T_c$ (0) if $m = m'$ (otherwise), (27) becomes

$$2\sigma^2_{noise}(n)=\frac{2N_0}{N_cT_c}\frac{1}{SF^2}\sum_{b=0}^{D-1}\varepsilon_b\sum_{k=nSF}^{(n+1)SF-1}\sum_{m=0}^{M-1}\left|w^{(m)}_{b\_u(j)}(k)\right|^2. \tag{28}$$

Hence, using (24), (26) and (28), the variance of μ can be rewritten as

$$\begin{aligned}2\sigma^2_{\mu} &= \frac{2}{SF^2}\frac{N_0}{N_cT_c}\\ &\times\Bigg[\sum_{b=0}^{D-1}\varepsilon_b\sum_{k=nSF}^{(n+1)SF-1}\sum_{m=0}^{M-1}\left|w^{(m)}_{b\_u(j)}(k)\right|^2\\ &+\frac{E_s}{N_0}\sum_{b=0}^{D-1}\varepsilon_b(U+\delta u_b-1)r^{-\alpha}_{b\_u(j)}10^{-\eta_{b\_u(j)}/10}\\ &\times\left\{\frac{1}{SF}\sum_{k=nSF}^{(n+1)SF-1}\left|\hat{H}_{b\_u(j)}(k)\right|^2-\left|\frac{1}{SF}\sum_{k=nSF}^{(n+1)SF-1}\hat{H}_{b\_u(j)}(k)\right|^2\right\}\\ &+\frac{E_s}{N_0}\sum_{b=0}^{D-1}\varepsilon_b\sum_{\substack{i=0\\ \neq b}}^{\infty}(U+\delta u_i)r^{-\alpha}_{i\_u(j)}10^{-\eta_{i\_u(j)}/10}\\ &\times\frac{1}{SF}\sum_{k=nSF}^{(n+1)SF-1}\sum_{m=0}^{M-1}\left|w^{(m)}_{b\_u(j)}(k)H^{(m)}_{i\_u(j)}(k)\right|^2\Bigg].\end{aligned} \tag{29}$$

To derive the conditional BER and evaluate the performance of the MC-CDMA downlink with site diversity operation, the conditional signal-to-interference plus noise (SINR) is defined. The conditional SINR can be expressed as

$$\gamma\left(E_s/N_0|\left\{H^{(m)}_{i\_u(j)}(k)\right\}\right)=\frac{\left|E\left[y_{u(j)}(n)|\left\{H^{(m)}_{i\_u(j)}(k)\right\}\right]\right|^2}{\sigma^2_{\mu}} \tag{30}$$

where

$$E\left[y_{u(j)}(n)|\{H^{(m)}_{i\_u(j)}(k)\}\right]=x_{u(j)}(n) \tag{31}$$

which is given by (13). Applying (29) and (31) to (30), the simplified conditional SINR is then given as

$$\begin{aligned}&\gamma\left(E_s/N_0|\{H^{(m)}_{i\_u(j)}(k)\}\right)\\ &=2SF\left(\frac{E_s}{N_0}\right)\left|\sum_{b=0}^{D-1}\varepsilon_b\sqrt{r^{-\alpha}_{b\_u(j)}10^{-\eta_{b\_u(j)}/10}}\right.\\ &\left.\frac{1}{SF}\sum_{k=nSF}^{(n+1)SF-1}\hat{H}_{b\_u(j)}(k)\right|^2\Bigg/\Bigg[\sum_{b=0}^{D-1}\varepsilon_b\sum_{k=nSF}^{(n+1)SF-1}\sum_{m=0}^{M-1}\left|w^{(m)}_{b\_u(j)}(k)\right|^2\\ &+\frac{E_s}{N_0}\sum_{b=0}^{D-1}\varepsilon_b(U+\delta u_b-1)r^{-\alpha}_{b\_u(j)}\times10^{-\eta_{b\_u(j)}/10}\\ &\times\left\{\frac{1}{SF}\sum_{k=nSF}^{(n+1)SF-1}\left|\hat{H}_{b\_u(j)}(k)\right|^2-\left|\frac{1}{SF}\sum_{k=nSF}^{(n+1)SF-1}\hat{H}_{b\_u(j)}(k)\right|^2\right\}\\ &+\frac{E_s}{N_0}\sum_{b=0}^{D-1}\varepsilon_b\sum_{\substack{i=0\\ \neq b}}^{\infty}r^{-\alpha}_{i\_u(j)}\times10^{-\eta_{i\_u(j)}/10}\times(U+\delta u_i)\\ &\times\frac{1}{SF}\sum_{k=nSF}^{(n+1)SF-1}\sum_{m=0}^{M-1}\left|w^{(m)}_{b\_u(j)}(k)H^{(m)}_{i\_u(j)}(k)\right|^2\Bigg].\end{aligned} \tag{32}$$

The downlink capacity performance can almost be explained from the above conditional SINR expression. When the number of active BS's selected is very small due to a small threshold P_{th}, the desired signal power reduces and this results in a lower SINR value. Therefore, a better SINR value is achieved by increasing the threshold value. On the other hand, with too large a threshold P_{th}, more active BS's are selected and this improves the desired signal power. However, the number of active channels is also increased due to site diversity operation, resulting in excessive MAI and ICI. This also degrades the SINR. Therefore, as previously mentioned, there should be an optimum P_{th} that can simultaneously improve the desired signal power and compensate the large interference components due to the increase of number of active channels.

3.2 Expression for Conditional BER and Local Average BER

The conditional BER for user $u(j)$ in cell of BS j is derived. The QPSK data modulation is considered. We assume all "1" transmission for user $u(j)$, i.e., $\{d_{u(j)}(n)=(1+j1)/\sqrt{2}\}$, but random binary data transmission for all other users. Based on the Gaussian approximation of the MAI and ICI components, the conditional BER for the given set of channel gains $\{H^{(m)}_{i\_u(j)}(k);\ k=0\sim N_c-1;\ m=0\sim M-1;\ i=0\sim\infty\}$ can be expressed as

$$\begin{aligned}&P_e[\gamma(E_s/N_0|\{H^{(m)}_{i\_u(j)}(k)\}]\\ &=\frac{1}{2}\Pr\left[\mathrm{Re}\left[y_{u(j)}(n)\right]<0|\{H^{(m)}_{i\_u(j)}(k)\}\right]\\ &\quad+\frac{1}{2}\Pr\left[\mathrm{Im}\left[y_{u(j)}(n)\right]<0|\{H^{(m)}_{i\_u(j)}(k)\}\right]\\ &=\frac{1}{2}erfc\left(\sqrt{\frac{\gamma(E_s/N_0|\{H^{(m)}_{i\_u(j)}(k)\}}{4}}\right),\end{aligned} \tag{33}$$

where $erfc(x)$ is the complementary error function given by $erfc(x)=\frac{2}{\sqrt{\pi}}\int_x^{\infty}\exp(-t^2)dt$. The theoretical local average BER for the transmitted nth modulated symbol can be numerically computed by averaging (33) over the given set of channel gains and written as

$$\begin{aligned}P_e\left(\frac{E_b}{N_0}\right)=&\int_0^{\infty}\cdots\int_0^{\infty}P_e[\gamma(E_s/N_0|\{H^{(m)}_{i\_u(j)}(k)\})]\\ &\times p(\{H^{(m)}_{i\_u(j)}(k)\})\prod_{m,k,i}dH^{(m)}_{i\_u(j)}(k)\end{aligned} \tag{34}$$

where $p(\{H^{(m)}_{i\_u(j)}(k)\})$ is the joint probability density function of $\{H^{(m)}_{i\_u(j)}(k)\}$. Accordingly, the downlink performance can then be examined.

4. Numerical Results and Discussion

In this section, the numerical computation for the local average BER is performed using the conditional BER expression. Then, the theoretical downlink capacity is obtained and compared to the computer simulation result.

4.1 Monte-Carlo Numerical Process

The evaluation of the downlink capacity is performed by the Monte-Carlo numerical method. The cellular structure and the computation condition are respectively shown in Table 1 and Fig. 3. An MC-CDMA system with N_c=256 subcarriers is assumed. The signal is assumed to propagate through a block Rayleigh fading channel having an L=16-path exponential power delay profile with decay factor γ dB and $\tau_l = l$, $l = 0 \sim L-1$. The shadowing loss standard deviation β is varied from 0 to 10 dB. An interference-limited environment is assumed such that the effect of the AWGN is neglected. The transmitted E_s/N_0 in (10) is set to 50 dB and the cell radius is normalized to unity. The interference coming from the second-tier cells is relatively weak and can be neglected [14]. Therefore each user will receive the dominant interference from the six adjacent cells' BS's. The user of interest is located in cell of BS 0 and there are 18 surrounding cells considered as co-channel cells. The maximum number D of active BS's is varied from 1 to 7, where D=1 corresponds to the no site diversity operation and D=7 corresponds to the site diversity operation with six adjacent co-channel cells.

The Monte-Carlo computation flowchart is summarized in Fig. 4. In each computation loop, the users' locations are randomly generated and this followed by the generation of path and shadowing losses for each user. For site diversity operation, the active BS's for each user are selected based on the local average signal-to-noise power ratio (SNR) and the threshold P_{th}. The number of active channels for each BS is then determined. Next the set of fading channel gains and the FDE weight for downlink transmission

Table 1 Computation condition.

MC-CDMA	Data modulation		QPSK
	No. of subcarriers		N_c=256
	Spreading factor		SF=256
	No. of receive antennas		M=1~4
	FDE		MMSE
Site diversity	Required BER		10^{-2}
	Allowable outage probability		0.1
	Maximum allowable no. of active BS's		D=1~7
	Threshold power		P_{th}=0~10dB
Channel model	Path loss exponent		α=3~4
	Shadowing loss standard deviation		β=4~10 dB
	Rayleigh fading	No. of paths	L=16
		Power delay profile	Exponential
		Decay factor	γ =0~10 dB

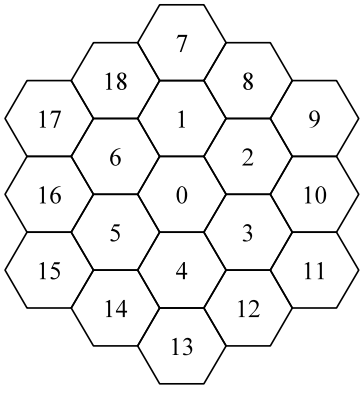

Fig. 3 Cellular structure.

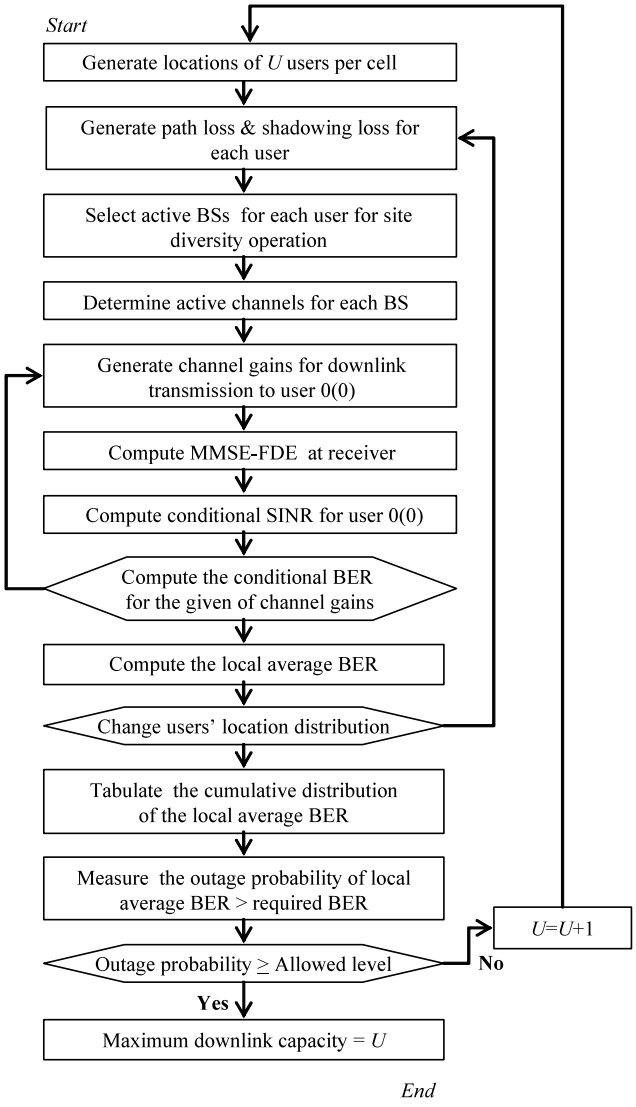

Fig. 4 Monte-Carlo numerical computation flowchart.

to user 0(0) are generated. Then the conditional SINR and BER are computed. The local average BER is tabulated with the locations for users randomly changed in every repeated computation loop. The outage probability (the probability of the local average BER larger than the required BER) is obtained using the cumulative distribution of the local average BER. As seen from Table 1, the required BER is 10^{-2} with the allowable outage probability given as 0.1. Then, the maximum number U of users per cell that satisfies the allowable outage probability is determined as the downlink capacity.

4.2 Confirming Gaussian Approximation

In Sect. 3, the interference components have been approximated as the complex-valued Gaussian random variables for computing the conditional SINR and BER. In Fig. 3, the probability density functions (pdf's) of the MAI and ICI components obtained from Gaussian approximation using theoretically derived variances, $2\sigma^2_{MAI}$ and $2\sigma^2_{ICI}$, are plotted. To verify this Gaussian approximation, the pdf's of the MAI and ICI components obtained from the computer simulation [10] are examined and plotted in Fig. 5. A uniform power delay profile for the channel (γ=0 dB) and 27 users per cell (U=27) are assumed. $P_{\rm th}$=4.5 dB is used for the case with site diversity operation. Only the real parts of μ_{MAI} and μ_{ICI} are plotted in Fig. 5. The computer simulation plots show that the pdf's of the real part of μ_{MAI} and μ_{ICI} follow the Gaussian distribution with zero-mean. This therefore justifies the approximation used in the theoretical analysis.

4.3 Numerical Results

The following numerical results from the theoretical computation show the impacts of various parameters: the threshold $P_{\rm th}$, the path loss exponent α, the shadowing loss standard deviation β, the number of maximum allowable number D of active BS's and the number M of receive antennas. Finally, the effect of the decay factor γ of the power delay profile is also examined.

Computer simulation results taken from [10] are also shown for comparison. The users' locations are also randomly distributed in each computer simulation run of [10]. After generation of path losses and shadowing losses, active BS's are selected based on the local average SNR for each user in site diversity operation. Users' data are then modulated and transmitted through a Rayleigh fading channel with L=16 paths. At the receiver, the site diversity operation is carried out, followed by data-demodulation and the number of transmission error is counted to measure the local average BER.

4.3.1 Effect of Site Diversity Threshold

The effect of site diversity threshold $P_{\rm th}$ on the downlink capacity, normalized by SF, is shown in Fig. 6. The uniform

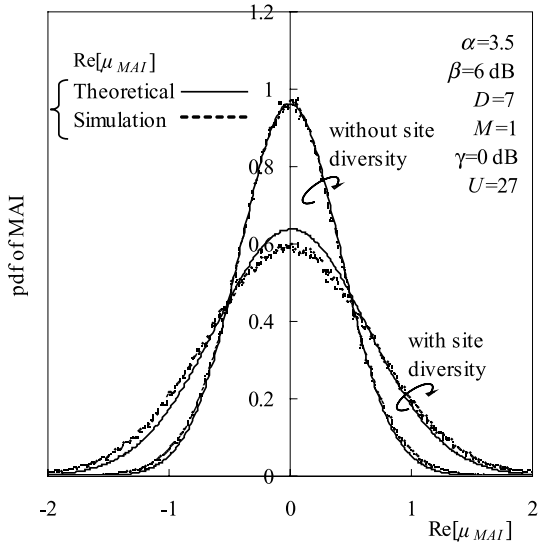

(a) MAI component.

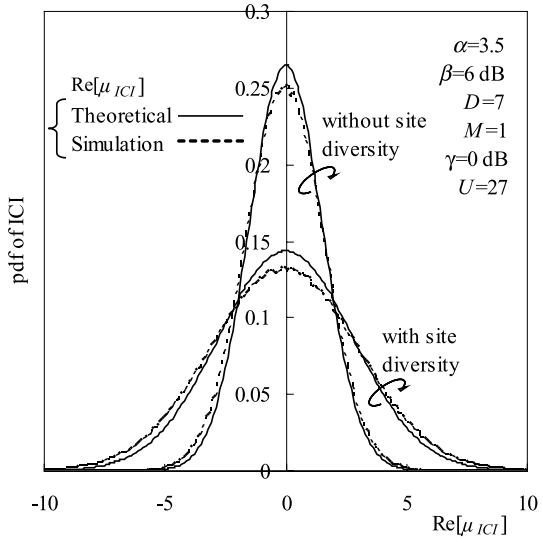

(b) ICI component.

Fig. 5 Distributions of MAI and ICI components.

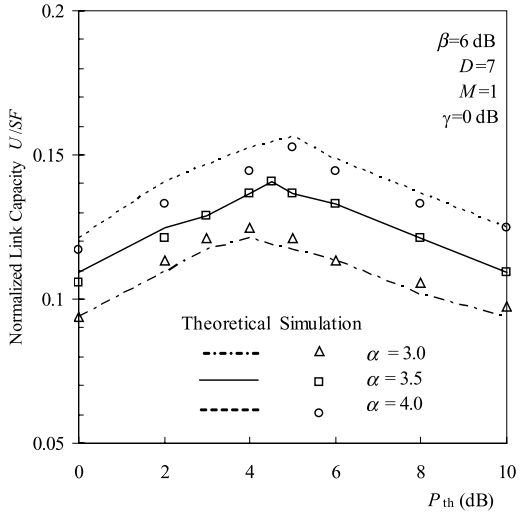

Fig. 6 Effect of site diversity threshold $P_{\rm th}$.

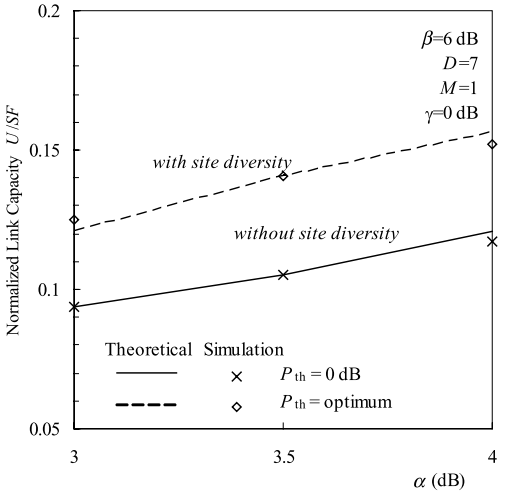

Fig. 7 Effect of path loss exponent α.

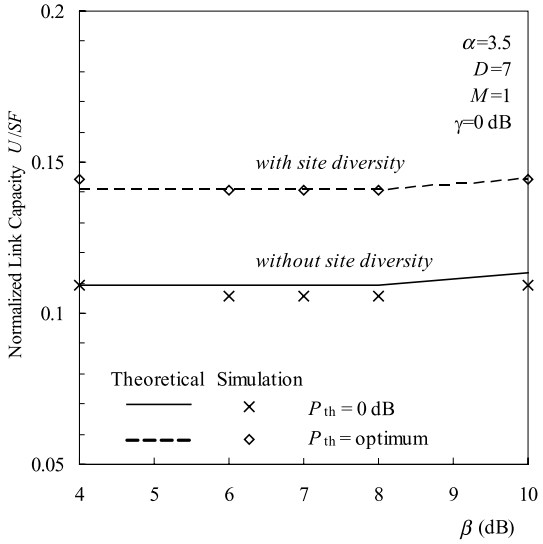

Fig. 8 Effect of shadowing loss standard deviation β.

power delay profile (γ=0 dB) is assumed. It is seen that the optimum P_{th} exists. As P_{th} increases from 0 dB to optimum, more active BS's are selected, and this gives higher SINR and better BER performance. Higher downlink capacity is thus obtained. However, as P_{th} becomes larger, the number of site diversity users is increased, creating excessive MAI and ICI despite of the improved received signal power. As a result, the downlink capacity is reduced. Therefore, controlling the P_{th} is very important for obtaining the appropriate number of active BS's to improve the BER performance for a mobile user and compensating the increase of MAI and ICI due to more additional active channels.

The optimum P_{th} becomes larger as path loss exponent α increases in both plots. This is because the received signal power decreases as α increases and causes the need for more active BS's in the site diversity operation. A fairly good agreement between the theoretical computation and computer simulation results are seen in Fig. 6.

4.3.2 Effects of Path Loss Exponent α and Shadowing Loss Standard Deviation β

Figures 7 and 8 show the effect of path loss exponent α and shadowing loss standard deviation β on the downlink capacity. For the case with site diversity operation, the optimum P_{th} is used, while P_{th}=0 dB (or D=1) for the case with no site diversity operation. In Fig. 7, the downlink capacity increases as α increases. Since path loss is proportional to the inverse α-th power of the distance, the interference power from relatively far BS's is greatly attenuated in comparison to the desired signal component from active BS's as α increases. This results in better SINR and thus, produces higher downlink capacity in the interference-limited environment.

It is seen from Fig. 8 that the downlink capacity performance is almost unaffected by the increase of β in both cases. As β increases, the variations in the interference power become larger and results in a higher probability of large interference, reducing the downlink capacity. However, since the interference power variations from different BS's are independent, the site diversity effect due to more active BS's selection increases and thus improves the received signal power. This compensates for the minor variations in the effect of β. In both figures, theoretical computation result shows a fairly good agreement with the computer simulation result.

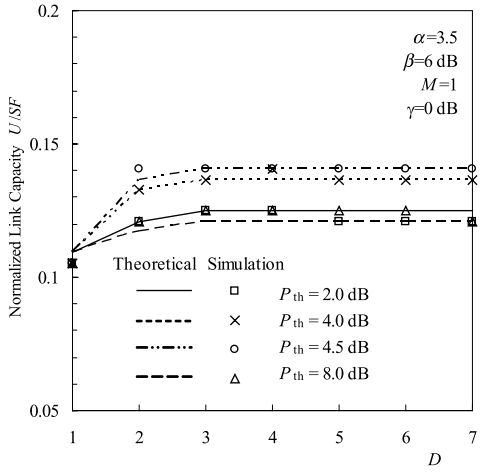

Fig. 9 Effect of maximum allowable number D of active BS's.

4.3.3 Effect of the Maximum Number D of Active BS's

Until now, a maximum allowable number D of active BS's is assumed to be D=7. The downlink capacity performance also depends on D. Figure 9 shows that as D increases, the downlink capacity increases, due to the higher site diversity effect. However, since more additional channels are necessary for site diversity operation, the interference power increases and the downlink capacity is reduced. Thus, there is a maximum achievable downlink capacity for each D. Ap-

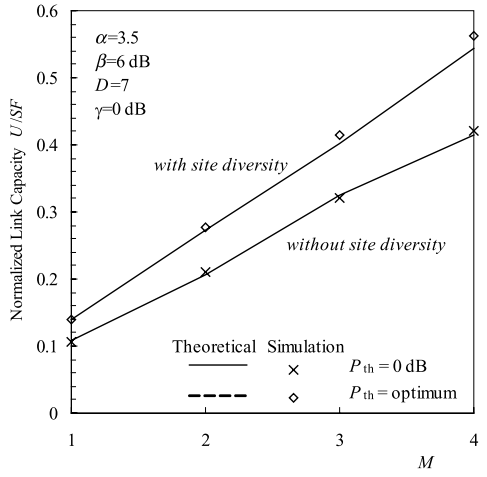

Fig. 10 Effect of number M of receive antennas.

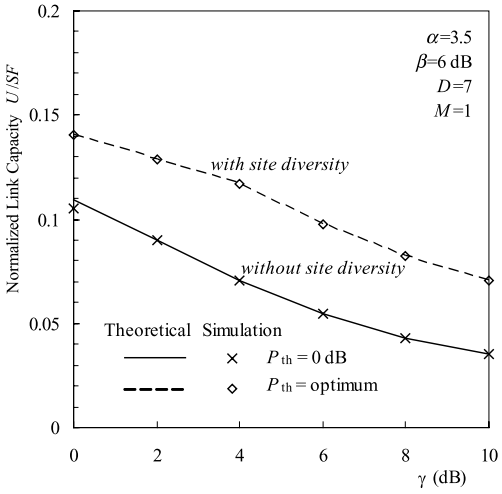

Fig. 11 Effect of decay factor γ.

parently, the maximum achievable value for different P_{th} lies in the region of D=3∼7, as shown in both theoretical computation and actual simulation plots. The theoretical computation plot exhibits similar characteristic in comparison to the computer simulation plot. It can be concluded that the maximum achievable downlink capacity can be obtained at D=3.

4.3.4 Performance Improvement by Antenna Diversity Reception

The single antenna reception has been assumed in the previous cases. Figure 10 shows the downlink capacity improvement by employing the antenna diversity reception. The downlink capacity increases almost linearly with the number M of receive antennas, both shown in theoretical computation and computer simulation plots.

4.3.5 Effect of Decay Factor γ of Exponential Power Delay Profile

The effect of decay factor γ of the exponential power delay profile channel is also examined.

From Fig. 11, as γ increases, the frequency-selectivity of the channel becomes weaker, thus reducing the frequency-diversity effect in MC-CDMA system. This degrades both the SINR and BER performance, resulting in reduced downlink capacity performance, despite the use of site diversity operation. Similar performance degradation is shown for both theoretical computation and computer simulation plots.

5. Conclusion

In this paper, a theoretical treatment was developed for the downlink site diversity reception with joint use of MMSE-FDE and antenna diversity in a MC-CDMA cellular system. The expressions for the conditional SINR and BER were derived based on Gaussian approximation of the interference components; and the local average BER was numerically computed using Monte-Carlo computation method. The theoretical performance results were compared with computer simulation results to show a high degree of agreement. It should also be pointed out that the theoretical evaluation has the advantage of taking less time in computation. Evidently, from both theoretical and simulation evaluations, the site diversity operation improves the MC-CDMA downlink performance. Both results showed that three (D=3) active BS's participating in site diversity operation are sufficient for achieving the maximum downlink capacity.

The theoretical analysis and computer simulation only considered the downlink case and for future work, the uplink site diversity reception should be studied for MC-CDMA cellular system. Further works can include finding a way to balance the optimum P_{th} and capacities for both link transmissions. Theoretical analysis on joint use with turbo-coded space-time transmit diversity (STTD) [15] can lead to a further interesting research.

References

[1] W.C. Jakes, Jr., ed., Microwave mobile communications, Wiley, New York, 1974.
[2] S. Hara and R. Prasad, "Overview of multicarrier CDMA," IEEE Commun. Mag., vol.35, no.12, pp.126–144, Dec. 1997.
[3] S. Hara and R. Prasad, "Design and performance of multicarrier CDMA system in frequency-selective Rayleigh fading channel," IEEE Trans. Veh. Technol., vol.48, no.5, pp.1584–1595, Sept. 1999.
[4] M. Helard, R. Le Gouable, J.F. Helard, and J.-Y. Beaudis, "Multicarrier CDMA techniques for future wideband wireless networks," Ann. Telecommun., vol.56, pp.260–274, 2001.
[5] N. Maeda, H. Atarashi, S. Abeta, and M. Sawahashi, "Antenna diversity reception appropriate for MMSEC combining in frequency domain for forward link OFCDM packet wireless access," IEICE Trans. Commun., vol.E85-B, no.10, pp.1966–1977, Oct. 2002.
[6] H. Atarashi, S. Abeta, and M. Sawahashi, "Variable spreading

factor-orthogonal frequency and code division multiplexing (VSF-OFCDM) for broadband packet wireless access," IEICE Trans. Commun., vol.E86-B, no.1, pp.291–299, Jan. 2003.

[7] F. Adachi and T. Sao, "Comparative study of various frequency equalization techniques for downlink of a wireless OFDM-CDMA system," IEICE Trans. Commun., vol.E86-B, no.1, pp.352–364, Jan. 2003.

[8] F. Adachi and T. Sao, "Joint antenna diversity and frequency-domain equalization for multi-rate MC-CDMA," IEICE Trans. Commun., vol.E86-B, no.11, pp.3217–3224, Nov. 2003.

[9] A.J. Viterbi, CDMA: Principles of spread spectrum communications, Addison Wesley, 1995.

[10] T. Inoue, S. Takaoka, and F. Adachi, "Frequency-domain equalization for MC-CDMA downlink site diversity and performance evaluation," IEICE Trans. Commun., vol.E88-B, no.1, pp.84–92, Jan. 2005.

[11] F. Adachi, M. Sawahashi, and H. Suda, "Wideband DS-CDMA for next generation mobile communications systems," IEEE Commun. Mag., vol.36, no.9, pp.56–69, Sept. 1998.

[12] C. Kchao and G.L. Stuber, "Analysis of a direct-sequence spread spectrum cellular radio system," IEEE Trans. Commun., vol.41, no.10, pp.1507–1516, Oct. 1993.

[13] J.G. Proakis, Digital communications, 4th ed., McGraw Hill, New York, 2000.

[14] W.C.Y. Lee, Mobile communications engineering: Theory and applications, 2nd ed., McGraw Hill, New York, 1997.

[15] S. Tsumura, M. Vehkapera, Z.L. Li, D. Tujkovic, M. Juntti, and S. Hara, "Performance evaluation of turbo and space-time turbo coded MC-CDMA downlink in single and multi-cell environments," IEICE Trans. Commun., vol.E87-B, no.10, pp.3011–3019, Oct. 2004.

Arny Ali was born in Malaysia in 1976. She received her B.Sc. (Electrical Engineering) from the George Washington University, Washington D.C. in 1999 and M.Eng. (Electrical & Communication Engineering) from the Tohoku University, Japan in 2005. She worked for TM Telekom Malaysia after graduation in 1999 as network application engineer, and later joined the Multimedia University in 2002 as assistant lecturer before pursuing the Master degree. Currently, she is a researcher at TM R&D (previously known as Telekom R&D) and attached to the Antenna Propagation Unit. Her research interest includes wireless and mobile communication systems, digital signal processing, multiple access technologies, and antenna propagation.

Takamichi Inoue received his B.E. and M.E. degrees in communications engineering from the Dept. of Electrical and Communications Engineering, Tohoku University, Sendai, Japan, in 2003 and 2005, respectively. He joined System Platforms Research Laboratories, NEC Corporation in 2005. He is engaged in research for beyond 3G mobile communications systems.

Fumiyuki Adachi received the B.S. and Dr. Eng. degrees in electrical engineering from Tohoku University, Sendai, Japan, in 1973 and 1984, respectively. In April 1973, he joined the Electrical Communications Laboratories of Nippon Telegraph & Telephone Corporation (now NTT) and conducted various types of research related to digital cellular mobile communications. From July 1992 to December 1999, he was with NTT Mobile Communications Network, Inc. (now NTT DoCoMo, Inc.), where he led a research group on wideband/broadband CDMA wireless access for IMT-2000 and beyond. Since January 2000, he has been with Tohoku University, Sendai, Japan, where he is a Professor of Electrical and Communication Engineering at the Graduate School of Engineering. His research interests are in CDMA wireless access techniques, equalization, transmit/receive antenna diversity, MIMO, adaptive transmission, and channel coding, with particular application to broadband wireless communications systems. From October 1984 to September 1985, he was a United Kingdom SERC Visiting Research Fellow in the Department of Electrical Engineering and Electronics at Liverpool University. He was a co-recipient of the IEICE Transactions best paper of the year award 1996 and again 1998 and also a recipient of Achievement award 2003. He is an IEEE Fellow and was a co-recipient of the IEEE Vehicular Technology Transactions best paper of the year award 1980 and again 1990 and also a recipient of Avant Garde award 2000. He was a recipient of Thomson Scientific Research Front Award 2004.